

LOW ALPHA OPERATION OF THE DIAMOND STORAGE RING

I.P.S. Martin^{1,2}, R. Bartolini^{1,2}, G. Rehm¹, J. H. Rowland¹, C. Thomas¹

¹Diamond Light Source Ltd, Harwell Innovation Campus, UK

²John Adams Institute, University of Oxford, UK

Abstract

The Diamond storage ring has been operated in low-alpha mode providing short-pulse radiation for pump-probe experiments and coherent radiation for THz/IR measurements. Two lattices have been implemented, with both capable of providing a variable alpha in the range $\pm 2 \times 10^{-5}$, down to minimum values well below 1×10^{-6} . The second lattice additionally provides a low emittance of 4nm.rad, compared to 35nm.rad for the first lattice. An overview of operation in low-alpha mode is given, along with first measurements of coherent emission at long wavelengths under a variety of conditions.

INTRODUCTION

The Diamond storage ring was first operated in a dedicated low-alpha mode during April 2009 to produce short-pulse radiation for pump-probe experiments [1]. As a result of this trial it was identified that the quality of experimental data taken in this mode would be considerably enhanced if the emittance of the electron beam could be brought closer to the value used during standard user operation. As such, a new low emittance low alpha lattice has been developed which retains the ability to smoothly vary the first-order momentum compaction factor (MCF), α_1 , without significantly altering the emittance of the ring.

LATTICE DESCRIPTION

The first order MCF and horizontal emittance of a storage ring are both defined by the variation of the linear dispersion η_1 in regions of non-zero bend radius:

$$\alpha_1 = \frac{1}{L} \oint \frac{\eta_1(s)}{\rho(s)} ds \quad (1)$$

$$\varepsilon = \frac{55}{32\sqrt{3}} \frac{\hbar \gamma^2}{m_e c} \frac{I_5}{I_2 - I_4} \quad (2)$$

where I_2 , I_4 and I_5 are the synchrotron radiation integrals containing the information of how the dispersion varies in the bending magnets. In order to reduce α_1 in the original low-alpha lattice design, the dispersion was made to cross from positive to negative values inside the bending magnets such that the integrated dispersion inside the magnets tends to zero and thus minimises equation (1). However, using this method the absolute dispersion remains large, resulting in the increased emittance.

In order to simultaneously reduce α_1 and ε , the new lattice achieves a low α_1 by retaining the quadratic dependence of the dispersion in the bending magnets of the standard user optics and only introducing negative

dispersion within the bending magnets themselves. In order to reach this solution the horizontal tune point has been increased from 21.150 for the original low-alpha lattice to 29.390 in the new lattice. This in turn has increased the natural chromaticity of the ring considerably, which combined with the reduction in dispersion at the sextupole locations has lead to a marked increase in the required sextupole strengths (S). This problem is compounded by the need to minimise the second order MCF (α_2) to maintain adequate momentum aperture [2]. This term is proportional to $\eta_1^3 S$ and is predominantly controlled by the focussing sextupoles in the centre of the arcs, where the peak dispersion is considerably reduced in the new lattice.

The optical functions for one super-period are given in figure 1 for the two lattices, and a summary of the main storage ring parameters in each case is given in table 1.

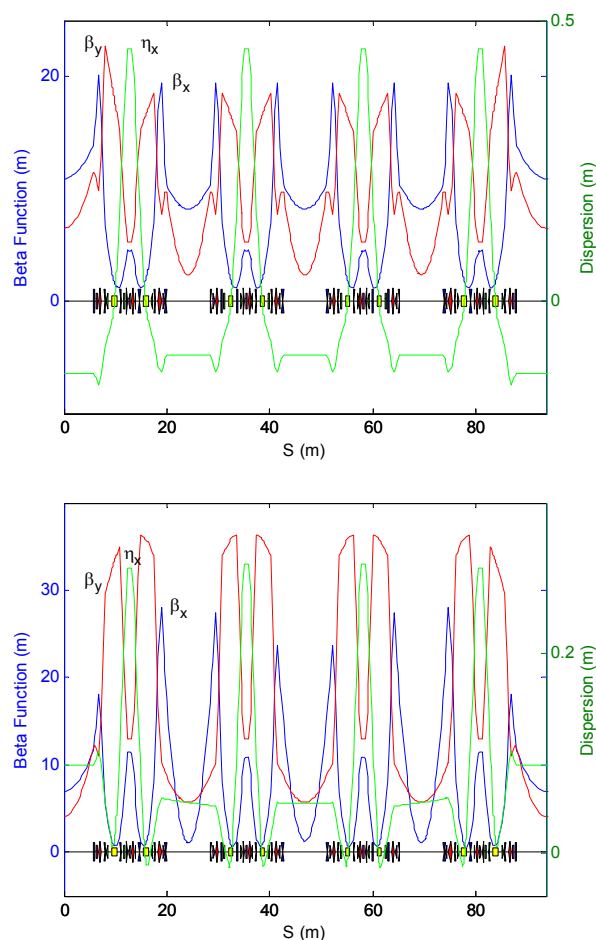


Figure 1: Optical functions for the high (top) and low (bottom) emittance low-alpha lattices.

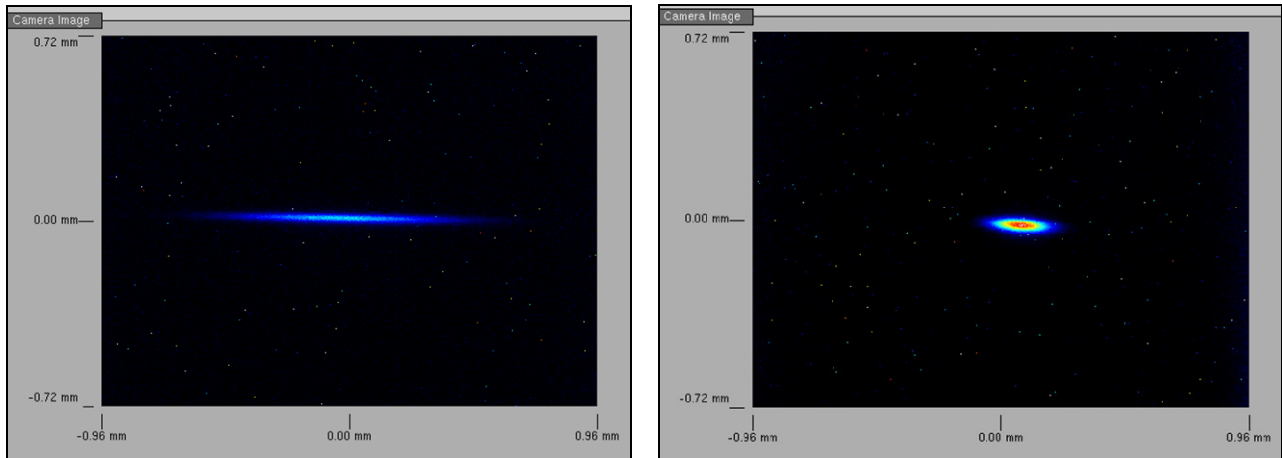


Figure 2: X-ray pinhole camera images comparing the electron beam size in the high (left) and low (right) emittance low-alpha lattices.

Table 1: Main Parameters of the Two Low Alpha Lattices

Parameter	High ϵ	Low ϵ
Emittance	35.2nm.rad	4.4nm.rad
α_1	-3×10^{-6}	-1×10^{-5}
α_2 (no sext.)	0.0116	0.0050
α_3	-0.0426	0.0040
Q_x / Q_y	21.150/12.397	29.390/8.284
Nat. chrom. (ζ_x / ζ_y)	-37 / -26	-66 / -43
$\beta_{xID} / \beta_{yID}$	8.2m / 2.4m	1.1m / 5.7m
Nat. bun. len (3MV)	1.3ps	2.4ps
Synch. freq. (3MV)	346Hz	629Hz

One further change with respect to the original low alpha lattice design is that a larger absolute value of α_1 has been targeted from the beginning. There are two main reasons for this decision. Firstly, whilst the larger α_1 gives a longer natural (zero-current) bunch length, the bunch length at moderate bunch currents rapidly becomes independent of α_1 , i.e. there is no benefit in further reducing α_1 once a minimum bunch length has been achieved at any given current [1]. Secondly, the transverse stability of the electron beam is found to be inversely proportional to α_1 , with strong orbit fluctuations observed dominated by a dispersive pattern. This reduced transverse stability acquires a new significance to users when the emittance of the beam is reduced, which relaxing the constraint on α_1 helps to address.

For both lattices a negative first order MCF was targeted from the beginning. In the original lattice this was to remove unwanted fixed points of motion in the longitudinal phase space caused by the MCF crossing zero at off-momentum values. It has not been possible to remove these fixed points in the new lattice; however, the negative MCF has been maintained in order to benefit from the reduced bunch-lengthening with current observed under these conditions [3].

MACHINE TRIALS

The new lattice was implemented and optimised during February 2010, with the beta-beat reduced to $\pm 2\%$ in both

planes following a LOCO correction [4]. Injection efficiency for the new lattice is typically in the range 30-40%, a marked improvement on the original, high emittance lattice.

Bunch Length Measurements

Measurements of bunch length as a function of current have been taken for both high and low emittance lattices under a variety of conditions. Figure 3 shows an example of one of these comparisons, in which α_1 was set to -6×10^{-6} and data measured for two RF cavity voltages. The bunch lengths were measured using a streak camera with an estimated dynamic point-spread function (PSF) of 2ps for a white beam, the precise value of which is still under study [5]. The bunch length measurements for the two lattices agree well up to 40 μA bunch current, above which the low emittance lattice becomes unstable and is observed to emit bursting radiation and rapidly lose charge.

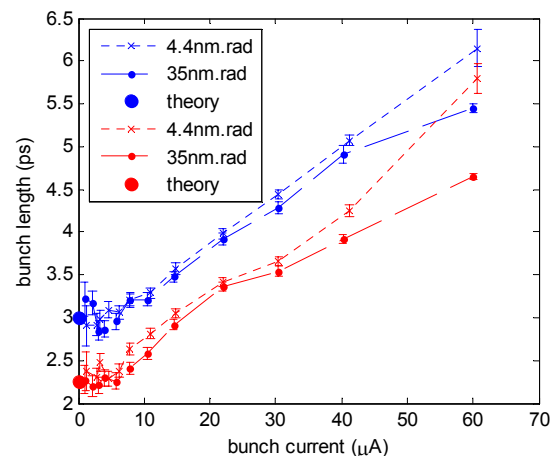


Figure 3: Comparison of bunch length as a function of current between the high and low emittance lattices. Data was measured at 1.5MV (blue) and 2.2MV (red).

As expected from the theory for negative MCF, an initial reduction in bunch length with increasing

current due to potential well distortion is observed before collective effects cause the bunch length to begin to grow again [3]. This bunch lengthening onset occurs at bunch currents of only a few μA , as can be seen in the data shown in figure 4. In this plot, bunch length measurements are presented for two values of α_l and for two RF cavity voltages, and it is clear that the reduction in bunch length with α_l at a given RF cavity voltage is only apparent for bunch currents below $\sim 10\text{-}20\mu\text{A}$. During low-alpha user runs the bunch current is set to $40\mu\text{A}$, justifying the decision to use a more relaxed value of α_l during these periods.

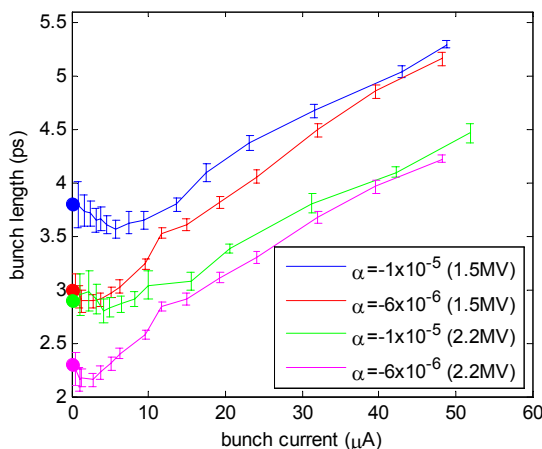


Figure 4: Bunch length as a function of current for two values of α_l . Data was measured at 1.5MV and 2.2MV. The natural bunch lengths predicted by theory are shown as coloured circles.

Coherent Emission

A further confirmation of the short bunch lengths achieved with this lattice can be found by observing the emission at wavelengths comparable to or longer than the bunch length, at which point the bunch is expected to emit coherently. The total power radiated by the electron bunch at a given wavelength can be derived from the power emitted by a single electron ($P_e(\lambda)$), the number of electrons in the bunch (n_e) and a form factor (f_λ) [6].

$$P(\lambda) = P_e(\lambda)(n_e + n_e(n_e - 1)f_\lambda)$$

The form factor f_λ is given by the square of the Fourier transform of the charge distribution and varies between 0 for an infinitely long bunch (incoherent emission) and 1 for a point-source (coherent emission). For large n_e (as is the case in electron storage rings), a clear indication that the emitted radiation is coherent is given if $P(\lambda)$ is found to be proportional to n_e^2 .

To detect coherent emission the Diamond storage ring is equipped with a Schottky Barrier Diode sensitive to the 60-90GHz bandwidth [7]. This detector has a fast response time of 250ps which allows the structure and evolution of the coherent emission to be studied on a turn-by-turn basis, albeit restricted to measuring mm-wave radiation longer than the expected bunch length.

The emitted radiation in this bandwidth was recorded for the same conditions to the bunch length measurements shown in figure 4 and is given in figure 5. There are three main points to note from this data. Firstly, the power radiated is confirmed to be proportional to I_b^2 up to the point where collective effects cause the bunch length to begin to grow. Secondly, the power emitted in this bandwidth at a given RF voltage is initially higher for a reduced value of α_l (when the bunch length is shorter), but as the current is increased and the bunch length becomes independent of α_l the emitted power also becomes independent of α_l . The last point to note is that in the time domain the radiation is emitted in a steady-state, i.e. the bunch current was kept below the bursting instability threshold.

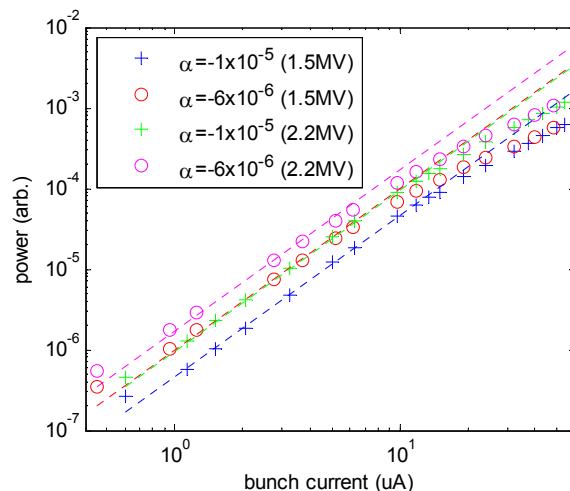


Figure 5: Power emitted in the 60-90GHz bandwidth as a function of current for two values of α_l . Data was measured at 1.5MV and 2.2MV.

CONCLUSIONS

A new low emittance, low-alpha lattice has been successfully commissioned for the Diamond storage ring and operated for users. The emittance of 4.4nm.rad compares favourably to the 2.7nm.rad supplied during standard operation. A campaign of measurements has begun for characterisation of the CSR emission, as it is anticipated there will be substantial gain for THz users in this mode of operation.

The authors gratefully acknowledge advice and encouragement from G. Wuestefeld and R. Walker during the course of this work.

REFERENCES

- [1] I. Martin et al., Proc PAC09 (2009)
- [2] D. Robin et al., Phys. Rev. E **48** 3 (1993)
- [3] S. Fang et al., KEK Preprint 94-190 (1995)
- [4] J. Safranek et al., NIM A **388**, 27 (1997)
- [5] C. Thomas et al., these proceedings
- [6] G. Wuestefeld et al., Proc EPAC08 (2008)
- [7] G. Rehm et al., Proc DIPAC09 (2009)